Title
Unidirectional hexagonal rare-earth disilicide nanowires on vicinal Si(100)-2×1

Journal
Applied Physics A, 80(6)

ISSN
0947-8396

Authors
Lee, D
Lim, DK
Bae, SS
et al.

Publication Date
2005-03-01

DOI
10.1007/s00339-004-3158-0

Appl. Phys. A 80, 1311–1313 (2005)
DOI: 10.1007/s00339-004-3158-0

Applied Physics A
Materials Science & Processing

D. LEE[1,✉]
D.K. LIM[1]
S.S. BAE[1]
S. KIM[1]
R. RAGAN[2]
D.A.A. OHLBERG[2]
Y. CHEN[2,3]
R. STANLEY WILLIAMS[2]

Unidirectional hexagonal rare-earth disilicide nanowires on vicinal Si(100)-2×1

[1] Department of Chemistry and School of Molecular Science (BK 21), Korea Advanced Institute of Science and Technology, Daejeon 305-701, Republic of Korea
[2] Quantum Science Research, Hewlett-Packard Laboratories, 1501 Page Mill Road, MS1123, Palo Alto, CA 94304, USA
[3] Department of Mechanical and Aerospace Engineering, University of California, Los Angeles, CA 90095, USA

Received: 14 September 2004/Accepted: 23 November 2004
Published online: 11 March 2005 •

ABSTRACT Rare-earth disilicide nanowires grown on vicinal Si(100) with a miscut of 2–2.5° toward the [110] azimuth at 600 °C were studied by scanning tunneling microscopy and compared with those grown on flat Si(001). In contrast to rare-earth disilicide nanowires grown on flat Si(100) surfaces, the nanowires grow unidirectionally along the [0$\bar{1}$1] direction of the vicinal Si(100) surface. Rare-earth disilicide nanowires form bundles composed of single nanowire units on both flat and vicinal surfaces. Yet, on the vicinal surface, the bundle width is comparable to the width of the terrace. The average nanowire length on the vicinal substrate is longer than that on the flat substrate. Scanning tunneling spectroscopy shows that the rare-earth disilicide nanowires have metallic properties.

PACS 81.07.Vb; 81.16.Dn; 68.65.La; 68.37.Ef

Nanometer-scale low-dimensional structures have generated much interest because of their potential applications in nano-electronic devices and biosensors. Confined electrons in low-dimensional metal-on-metal and semiconductor systems have been shown to have interesting electronic, transport, and magnetic properties [1–5]. Because of the high conductivity and extremely low Schottky barrier height on *n*-type Si, rare-earth disilicides ($RESi_{2-x}$s) are good candidates as conducting materials. Recently, hexagonal $RESi_{2-x}$ (RE = Dy [6, 7, 9], Er [8, 9], or Gd [9–11]) nanowires (NWs) have been prepared on flat Si(100) surfaces by utilizing the anisotropic lattice mismatches between the hexagonal $RESi_{2-x}$ and the Si substrate. These NWs were bidirectional and of limited length because of the double-domain structure of the Si(100) surface. However, if such NWs are to be used as interconnecting wires in nano-electronic devices, a fabrication method must be used that gives unidirectional, longer wires. We have grown ordered arrays of unidirectional self-assembled $ErSi_{2-x}$, Sm_3Si_5, and $DySi_{2-x}$ NWs with lengths exceeding 1 μm on vicinal Si(100) surfaces with a miscut of 2.5° off toward the [110] azimuth [12]. Another system that has recently been shown by Liu and Nogami to give long, unidirectional NWs is the growth of $GdSi_{2-x}$ NWs on a single-domain vicinal Si(100) surface with a miscut of 4° off toward the [110] azimuth [13]. However, their study focused on the conditions of $GdSi_{2-x}$ NW growth and did not elucidate the detailed structures of the resulting $GdSi_{2-x}$ NWs. In the present study, we chose to grow $GdSi_{2-x}$, $ErSi_{2-x}$, $DySi_{2-x}$, and Sm_3Si_5 NWs on a vicinal Si(100) surface with a miscut of 2–2.5° off toward the [110] azimuth (briefly, 'vicinal Si(100) surface') rather than a 4° off vicinal Si(100) surface to give unidirectional $RESi_{2-x}$ NWs with more stable width. In this letter, unidirectional hexagonal $GdSi_{2-x}$, $ErSi_{2-x}$, $DySi_{2-x}$, and Sm_3Si_5 NW formation on a vicinal Si(100) surface is investigated using scanning tunneling microscopy (STM) and scanning tunneling spectroscopy (STS). We gathered statistics on the average length and width of NWs on the vicinal Si(001) surface and compared this to the average length and width of NWs on flat Si(001) substrates [10]. The length of $RESi_{2-x}$ NWs on vicinal Si(001) is limited only by kinks or step bunches, and the maximum width is found to be correlated to the original terrace width on the vicinal Si(001) surface.

All experiments were performed in an ultra-high-vacuum (UHV) chamber with a base pressure of 1.0×10^{-10} Torr. The UHV chamber was equipped with an OMICRON VT-STM. Vicinal Si(100) surfaces with a resistivity of 1–10 Ω cm (Virginia Semiconductor) were cleaned by repeated flashing to 1200 °C after outgassing at 600 °C for longer than 3 h. The surface was confirmed to have a clean single-domain Si(100)-2 × 1 structure by STM at room temperature (RT). Rare-earth metal deposition and coverage-determination methods were explained elsewhere [10, 12]. In the constant current imaging mode at 0.1 nA, the sample bias voltage was set to be −2.0 V. All STM measurements were performed at RT.

Unlike the flat Si(100) surface, vicinal Si(100) surfaces with miscut angles larger than 1.5° consist of a single-domain 2 × 1 structure. As the Si(100) miscut angle increases, the portion of the surface covered by a single domain also increases. For example, the 4° off vicinal Si(100)-2 × 1 surface shows a double-height step structure with the single domain (> 95%) [14, 15]. The tendency to form a single-domain surface is attributed to the high stability of the double-height step with the direction of the dimer rows perpendicular to the step edges (D_B step) [14]. The STM image of the clean 2° (2.5°) off vicinal Si(100) surface exhibits well-ordered 2 × 1 terraces of average width 8.06 (6.15) nm, which corresponds to 21 (16) Si dimers along [011] separated by D_B steps. However, some S_A

✉ Fax: +82-42-868-5047, E-mail: dohyunlee@kaist.ac.kr

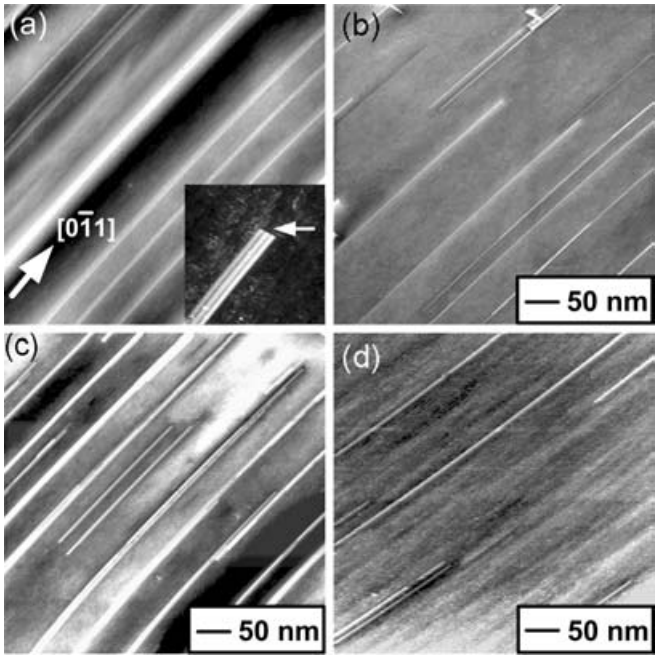

FIGURE 1 Filled-state STM image of unidirectional hexagonal $GdSi_{2-x}$ NWs (**a**) on the 2° off vicinal Si(100) surface (*inset*). The filled-state STM image shows the termination of NW growth by kink (10 nm × 10 nm). (**b**) $ErSi_{2-x}$ NWs, (**c**) $DySi_{2-x}$ NWs, (**d**) Sm_3Si_5 NWs on the 2.5° off vicinal Si(100) surface. $V_s = -2.0$ V, $I_t = 0.1$ nA with 500 nm × 500 nm

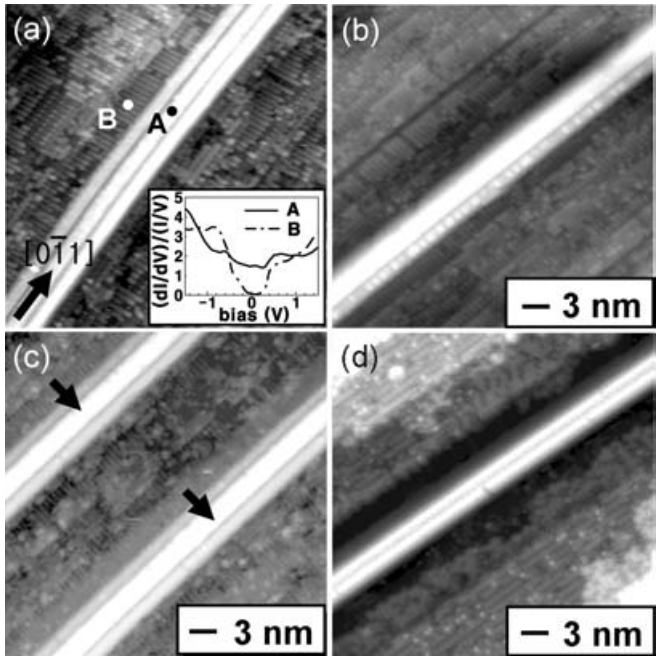

FIGURE 2 High-resolution STM images of (**a**) a bundle of single hexagonal $GdSi_{2-x}$ NWs. *Inset*: normalized STS spectra recorded at positions A, on top of the NWs, and B, the surrounding substrate area. (**b**) $ErSi_{2-x}$ NWs, (**c**) $DySi_{2-x}$ NWs, (**d**) Sm_3Si_5 NWs. $V_s = -2.0$ V, $I_t = 0.1$ nA with 35 nm × 35 nm

steps are also observed in the STM image due to the reduced step–step interaction [15].

Figure 1 shows filled-state STM images of (a) $GdSi_{2-x}$, (b) $ErSi_{2-x}$, (c) $DySi_{2-x}$, and (d) Sm_3Si_5 NWs formed by metal deposition at 600 °C with coverages of 0.33 ML Gd, 0.15 ML Er, 0.25 ML Dy, and 0.55 ML Sm, respectively. The samples are then annealed at 600 °C for two or more minutes. The STM images show that unidirectional $RESi_{2-x}$ NWs grow along the [0$\bar{1}$1] direction (parallel to the step edges of the vicinal Si(100) surface). This differs from the case of the flat Si(100) surface, on which bidirectional NW growth is observed due to the double-domain surface structures separated by single-height steps (S_A and S_B steps) [10]. The length of the unidirectional $RESi_{2-x}$ NWs on the vicinal Si(100) surface is only limited by kink angle – the accidental misorientation out of the phase defined by [100] and [011]. The inset of Fig. 1a clearly shows the termination of $GdSi_{2-x}$ NW growth by the kink of the vicinal Si(100) surface (marked by a white arrow). On the flat Si(100) surface, in contrast, the growth of $RESi_{2-x}$ NWs appears to be terminated when they encounter bunched steps or other perpendicularly grown NWs [10]. Therefore, the NW length is determined mainly by the NW density and the terrace width. On the vicinal Si(100) surface, however, $RESi_{2-x}$ NWs grow along [0$\bar{1}$1] without being interrupted by other NWs (as shown in Fig. 1). These NWs never cross each other. The average lengths of hexagonal $GdSi_{2-x}$ and $ErSi_{2-x}$ NWs grown on the flat Si(100) surface are 580 nm [10] and 472 nm [8], respectively. On the vicinal Si(100) surface, however, the average lengths of the hexagonal $GdSi_{2-x}$, $ErSi_{2-x}$, $DySi_{2-x}$, and Sm_3Si_5 NWs are 2100 nm, 1278 nm, 1345 nm, and 1300 nm, respectively. (We have calculated the average lengths and widths of four hexagonal $RESi_{2-x}$ NWs by counting 100 $GdSi_{2-x}$, 54 $ErSi_{2-x}$, 48 $DySi_{2-x}$, and 24 Sm_3Si_5 NWs from more than 10 STM images, respectively.) We therefore conclude that unidirectional hexagonal $RESi_{2-x}$ NWs with very high aspect ratios of the order of 1000 grow on the vicinal Si(100) surface. The lattice mismatch between hexagonal $GdSi_{2-x}$ (0.8 %), $ErSi_{2-x}$ (-1.6 %), $DySi_{2-x}$ (-0.1 %), Sm_3Si_5 (1.6%), and the Si substrate along one axis (*a* axis, $[11\bar{2}0]_{silicide}//[0\bar{1}1]_{Si}$) is low, whereas the lattice mismatch along the perpendicular axis (*c* axis, $[0001]_{silicide}//[011]_{Si}$) is quite high (8.9%, 6.3%, 7.6%, and 9.8%). This asymmetry in lattice mismatch favors growth of uniaxial nanostructures.

Magnified STM images of $RESi_{2-x}$ NWs are shown in Fig. 2. Figure 2a shows that $GdSi_{2-x}$ NWs are composed of a bundle of individual wires with average width of 2.1 nm, which corresponds to five unit cells of hexagonal $GdSi_{2-x}$ along the $[0001]_{silicide}//[011]_{Si}$ direction (5×0.42 nm $= 2.10$ nm). Previous studies have shown that bulk structures of Gd disilicide formed on Si(100) surfaces are either hexagonal $GdSi_{2-x}$ (AlB_2 type) or orthorhombic $GdSi_2$, depending on the growth temperature [16–18]. At a NW growth temperature of 600 °C, the hexagonal $GdSi_{2-x}$ structure is favored. The surface reconstruction of a single $GdSi_{2-x}$ NW is $c(2 \times 2)$, which is consistent with the hexagonal structure [10]. The hexagonal $GdSi_{2-x}$ unit cell has lattice constants of 0.39 nm along the $[11\bar{2}0]$ direction (*a* axis) and 0.42 nm along the [0001] direction (*c* axis). When the hexagonal $GdSi_{2-x}$ is grown pseudomorphically on Si(100) along the $[0001]_{silicide}//[011]_{Si}$ direction, the lattice mismatch between the hexagonal $GdSi_{2-x}$ and the Si substrate gradually increases to a maximum difference of half a unit cell at every sixth $GdSi_{2-x}$ (i.e. 6 × (lattice constant of $GdSi_{2-x}$)

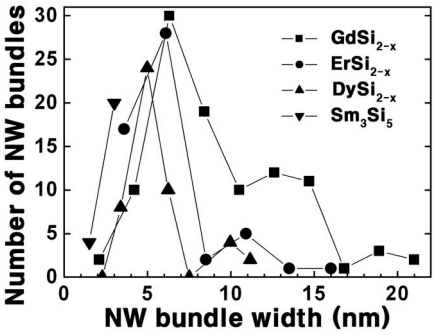

FIGURE 3 The number of single $RESi_{2-x}$ NWs in a NW bundle and NW bundle width distribution on the vicinal Si(100) surface

$= 6.5 \times$ (lattice constant of Si)). This gradual increase in lattice mismatch limits pseudomorphic lateral growth along the $[0001]_{\text{silicide}}//[011]_{\text{Si}}$ direction, and ultimately limits the width of coherently strained NWs in this direction to five hexagonal $GdSi_{2-x}$ unit cells (2.10 nm). In the perpendicular direction ($[11\bar{2}0]_{\text{silicide}}//[0\bar{1}1]_{\text{Si}}$), however, the lattice mismatch between hexagonal $GdSi_{2-x}$ and the Si substrate is only 0.9%. This lattice mismatch is sufficiently small that $GdSi_{2-x}$ NWs can grow to almost unlimited lengths along this direction. The inset of Fig. 2a shows normalized STS spectra recorded at two positions on the surface, specifically, on top of the hexagonal $GdSi_{2-x}$ NW (A) and on top of a Si dimer (B). Curve A shows a higher local conductivity near the Fermi level (zero bias) than curve B, indicating that the hexagonal $GdSi_{2-x}$ NW has metallic properties. A bundle of two $ErSi_{2-x}$ NWs are shown in Fig. 2b. The narrower 1.38 nm $ErSi_{2-x}$ NW is located near the wider 2.56 nm $ErSi_{2-x}$ NW as a satellite wire. In Fig. 2c, the structure of the $DySi_{2-x}$ NW highlighted with an arrow is composed of a single NW in the center with a width of 2.28 nm and satellite NWs with widths of 1.20 nm and 1.50 nm. In agreement with statistics gathered by Liu and Nogami, the width of $DySi_{2-x}$ NWs is quantized with respect to the $[011]_{\text{Si}}$ lattice constant [19]. In the case of Sm_3Si_5 NWs on Si(001) (Fig. 2d), the lattice mismatch along the $[011]_{\text{Si}}$ direction is large, 9.8%; thus, the NW width is narrow, 1.50 nm [12]. The maximum number of NWs forming a bundle in the Sm_3Si_5 on Si(001) system seen is two because of this large lattice mismatch. From the above observations, the single NW width is related to the lattice mismatch along the $[0001]_{\text{silicide}}//[011]_{\text{Si}}$ direction. The lateral widths of predominantly observed single $ErSi_{2-x}$, $DySi_{2-x}$, $GdSi_{2-x}$, and Sm_3Si_5 NWs are 2.70 nm, 2.28 nm, 2.10 nm, and 1.50 nm, which have an inverse relationship to the lattice mismatches along the $[0001]_{\text{silicide}}//[011]_{\text{Si}}$ direction (6.3%, 7.6%, 8.9%, and 9.8%).

The number of single $RESi_{2-x}$ NWs in a NW bundle and NW bundle width distribution are simultaneously shown in Fig. 3. The most frequently observed $GdSi_{2-x}$, $ErSi_{2-x}$, $DySi_{2-x}$, and Sm_3Si_5 NWs are bundles of three, two, three, and two single wires, with average bundle widths of 6.30 nm, 6.10 nm, 4.98 nm, and 3.00 nm, respectively (i.e. less than the width of the original terraces on the Si(100) surface, 8.06 nm (6.15 nm) on the 2° (2.5°) off vicinal Si(100) surface). The tendency to form bundles of these dimensions can be attributed to the high stability of the original terrace width due to step–step interaction, which causes NWs to form such that they maintain the original terrace width of the vicinal Si(100) surface at submonolayer coverages of rare-earth metal. (The average terrace width of Fig. 2a is 8.10 nm, and those of Fig. 2b–d are 6.10, 6.08, and 6.25 nm, respectively.) We can also suggest the exact dependence of the NW width distribution on terrace width by comparing Fig. 2a and Fig. 1b of [10]. They show the most frequently observed (typical) $GdSi_{2-x}$ NW grown on vicinal and flat Si(100) surfaces, respectively.

In summary, we have investigated the formation of unidirectional hexagonal $RESi_{2-x}$ NWs on a vicinal Si(100) surface. Unlike the case of a flat Si(100) surface, unidirectional hexagonal $RESi_{2-x}$ NWs were found to grow along the $[0\bar{1}1]$ direction of the vicinal Si(100) surface. Most significantly, the lengths of these NWs were longer than on a flat surface because of the absence of obstacles such as perpendicularly grown NWs or bunched steps as well as a low lattice mismatch. Single NWs had lateral widths as narrow as 1.20 nm, yielding an aspect ratio of 1000. The high aspect ratio of the NWs is due to anisotropic lattice mismatches between hexagonal $RESi_{2-x}$ and the single-domain vicinal Si substrate. Hexagonal $RESi_{2-x}$ NWs are formed as NW bundles on the vicinal Si(100) surface. The bundle width is dependent on the terrace width of vicinal Si(100). Thus, by appropriate selection of the Si substrate, we can exactly control the width of hexagonal $RESi_{2-x}$ NWs. Hexagonal $RESi_{2-x}$ NWs have metallic properties shown by STS, opening the possibility for their utilization in nano-electronic devices.

ACKNOWLEDGEMENTS This research was supported by grants from the KOSEF through the Center for Nanotubes and Nanostructured Composites, the Brain Korea 21 Project, the Advanced Backbone IT Technology Development Project of the Ministry of Information and Communication, and the National R&D project for nanoscience and nanotechnology. The research at Hewlett-Packard was supported in part by DARPA.

REFERENCES

1 M.F. Crommie, C.P. Lutz, D.M. Eigler: Nature (Lond.) **363**, 524 (1993)
2 F.J. Himpsel, J.E. Ortega: Phys. Rev. B **50**, 4992 (1994)
3 L. Bürgi, O. Jeandupeux, A. Hirstein, H. Brune, K. Kern: Phys. Rev. Lett. **81**, 5370 (1998)
4 S.S.P. Parkin, N. More, K.P. Roche: Phys. Rev. Lett. **64**, 2304 (1990)
5 F.J. Himpsel, J.E. Ortega, G.J. Mankey, R.F. Willis: Adv. Phys. **47**, 511 (1998)
6 C. Preinesberger, S. Vandrë, T. Kalka, S. Dahne-Prietsch: J. Phys. D: Appl. Phys. **31**, L43 (1998)
7 J. Nogami, B.Z. Liu, M.V. Katkov, C. Ohbuchi, N.O. Birge: Phys. Rev. B **63**, 233 305 (2001)
8 Y. Chen, D.A.A. Ohlberg, G. Medeiros-Ribeiro, Y.A. Chang, R.S. Williams: Appl. Phys. Lett. **76**, 4004 (2000)
9 Y. Chen, D.A.A. Ohlberg, R.S. Williams: J. Appl. Phys. **91**, 3213 (2002)
10 D. Lee, S. Kim: Appl. Phys. Lett. **82**, 2619 (2003)
11 J.L. McChesney, A. Kirakosian, R. Bennewitz, J.N. Crain, J.-L. Lin, F.J. Himpsel: Nanotechnology **13**, 545 (2002)
12 R. Ragan, Y. Chen, D.A.A. Ohlberg, G. Medeiros-Ribeiro, R.S. Williams: J. Cryst. Growth **251**, 657 (2003)
13 B.Z. Liu, J. Nogami: Nanotechnology **14**, 873 (2003)
14 D.J. Chadi: Phys. Rev. Lett. **59**, 1691 (1987)
15 B.S. Swartzentruber, N. Kitamura, M.G. Lagally, M.B. Webb: Phys. Rev. B **47**, 13 432 (1993)
16 G.L. Molnár, G. Petö, Z.E. Horváth, E. Zsoldos, N.Q. Khánh: Microelectron. Eng. **37–38**, 565 (1997)
17 S. Jin, H. Bender, M.F. Wu, A. Vantomme, H. Pattyn, G. Langouche: J. Appl. Phys. **81**, 3103 (1997)
18 J.C. Chen, G.H. Shen, L.J. Chen: Appl. Surf. Sci. **142**, 291 (1999)
19 B.Z. Liu, J. Nogami: J. Appl. Phys. **93**, 593 (2003)